Journal of Materials Processing Technology 155–156 (2004) 2039–2044

Journal of Materials Processing Technology

www.elsevier.com/locate/jmatprotec

Jet impingement onto a conical hole in relation to laser machining

B.S. Yilbas*, S.Z. Shuja, M.O. Budair

ME Department, KFUPM, Dhahran 31261, Saudi Arabia

Abstract

In the present study, laser heating process including the assisting gas jet is investigated numerically. Three-dimensional heating with assisting gas flow situation is modelled. Steel is employed in the simulations and air jet, as an assisting gas, is introduced impinging onto the workpiece surface coaxially with the laser beam. A numerical method using a control volume approach is introduced to solve continuity, momentum and energy equations in the fluid (air) side, while energy equation allowing conduction and phase change processes is solved in the solid region. The flow field is determined by solving the Navier–Stokes equation for compressible flow, and the turbulence effects are accounted for by the Reynolds stress turbulence (RSTM) model.

Keywords: Laser; Heating; Assisting gas; Jet

1. Introduction

Laser machining of engineering materials requires deep investigation into laser–workpiece interaction mechanism, which is generally complicated and depends on the laser and workpiece properties. In laser processing, an assisting gas jet is introduced coaxially with the laser beam. Assisting gas has two fold effects: (i) it shields the surface from the high temperature reactions and (ii) enhances the heating process through exothermic reactions. In the former case, assisting gas is inert such as argon while it is oxygen for the later case.

The heat transfer characteristics of a surface due to impinging jet were investigated extensively to explore the physical processes involved. A comprehensive review on heat transfer under impinging jets was carried out by Polat et al. [1]. They indicated that prediction of flow, heat, and mass transfer under a single, semi-confined turbulent jet might be employed as a good test for new turbulence models. A review of heat transfer data for single circular jet impingement was presented by Jambunathan et al. [2]. They suggested that the Nusselt number was independent of nozzle-to-plate spacing up to a value of 12 nozzle diameters at radii greater than nozzle diameters from the stagnation point. Heat transfer measurements from a surface with uniform heat flux and an impinging jet were studied by Baughn and Shimizu [3]. They showed that the maximum stagnation point heat transfer occurred for ratio of wall to nozzle spacing to nozzle diameter (z/D) of approximately 6. The effect of ambient air entrainment into a heated impinging jet on the heat transfer from a flat plate surface was investigated by Baughn et al. [4]. They indicated that it was possible to use heat transfer data for the heated jet, if the effectiveness was known and the local heat transfer coefficient was defined in terms of the adiabatic wall temperature. The local heat transfer coefficient distribution on a square heat source due to a normally impinging axisymmetric, confined, and submerged liquid jet was studied by Morris et al. [5]. They indicated that the predicted heat transfer coefficients were in good agreement with the experimental results. Turbulent planar jet impinging onto a slot was studied by Tchavdarov [6] using Chorin's random vortex method. He showed that the impinging vortex rebounds from the solid wall and a secondary vortex was ejected from the viscous layer. The characteristics of turbulent submerged axisymmetric incompressible jets impinging on a flat plate and flowing into axisymmetric cavity were studied by Amano and Brandt [7]. They showed that the velocity profile and the turbulence intensity at the nozzle exit affected the magnitude of the maximum skin friction on the wall.

In the present study, laser heating process including the assisting gas jet is investigated numerically. Two-dimensional axisymmetric heating with assisting gas flow situation is modelled. Steel is employed in the simulations and air jet, as an assisting gas, is introduced impinging onto the workpiece surface coaxially with the laser beam. A numerical method using a control volume approach is introduced to solve continuity, momentum and energy equations in the fluid (air) side, while energy equation allowing conduction and phase change processes is solved in the solid region.

* Corresponding author. Tel.: +966-3-860-2540; fax: +966-3-860-2949.
E-mail addresses: bsyilbas@kfupm.edu.sa (B.S. Yilbas), mobudair@kfupm.edu.sa (M.O. Budair).

0924-0136/$ – see front matter © 2004 Elsevier B.V. All rights reserved.
doi:10.1016/j.jmatprotec.2004.04.227

The flow field is determined by solving the Navier–Stokes equation for compressible flow, and the turbulence effects are accounted for by the Reynolds stress turbulence (RSTM) model. Gaussian profile is assumed for the spatial distribution of the laser output power intensity while time dependent profile resembling the laser output pulse is introduced in the computation for the non-conduction laser heating process. The thermal properties of the substance and assisting gas jet are considered as constant. Although the hole geometry is developed transiently during the laser heating process, the simplification of the problem is considered in the analysis. In this case, simulations are repeated for different cavity cone angles while keeping the wall temperature of the hole constant at about melting temperature of the substrate material.

2. Mathematical modelling

In the process industry, the impinging jet conditions are mainly steady; consequently, a steady flow conditions are considered in the analysis. The compressibility effect and variable properties are accommodated as well as temperature dependent thermal conductivity and specific heat are taken into account for the solid substance. The jet impinging onto the conical cavity with constant wall temperature (1500 K) situation is simulated for two jet velocities and four cavity depths. The geometric arrangement of the jet and the cavity in the solid substrate are shown in Fig. 1 while two cavity depths are considered, i.e. 0.5 and 1 mm.

2.1. Flow equations

The governing flow and energy equations for the axisymmetric impinging jet can be written in the Cartesian tensor notation as

- the continuity equation is

$$\frac{\partial}{\partial x_i}(\rho U_i) = 0 \tag{1}$$

- the momentum equation is

$$\frac{\partial}{\partial x_i}(\rho U_i U_j) = -\frac{\partial p}{\partial x_j} + \frac{\partial}{\partial x_i}\left[\mu\left(\frac{\partial U_i}{\partial x_j} + \frac{\partial U_j}{\partial x_i}\right) - \rho\overline{u_i u_j}\right] \tag{2}$$

In order to account for the turbulence, Reynolds stress model is employed. The mathematical details of the turbulence model is given in [8].

2.2. Flow boundary conditions

Four boundary conditions are considered in accordance with the geometric arrangement of the problem as shown in Fig. 1; they are as follows:

- *Solid wall*. No slip condition is assumed at the solid wall and the boundary condition for the velocity at the solid wall is zero.
- *Inlet conditions*. The boundary conditions for temperature and velocity need to be introduced at inlet. The values of k and ε are not known at the inlet, but can be determined from turbulent kinetic [9].
- *Outlet condition*. The flow is considered to be extended over a long domain; therefore, the boundary condition (unbounded boundaries, Fig. 1) for any variable ϕ is $\partial\phi/\partial x_i = 0$, where x_i is the normal direction at outlet.
- *Symmetry axis*. At the symmetry axis, the radial derivative of the variables is set to zero, except $V = \overline{vu} = \overline{vh} = \overline{wh}$.

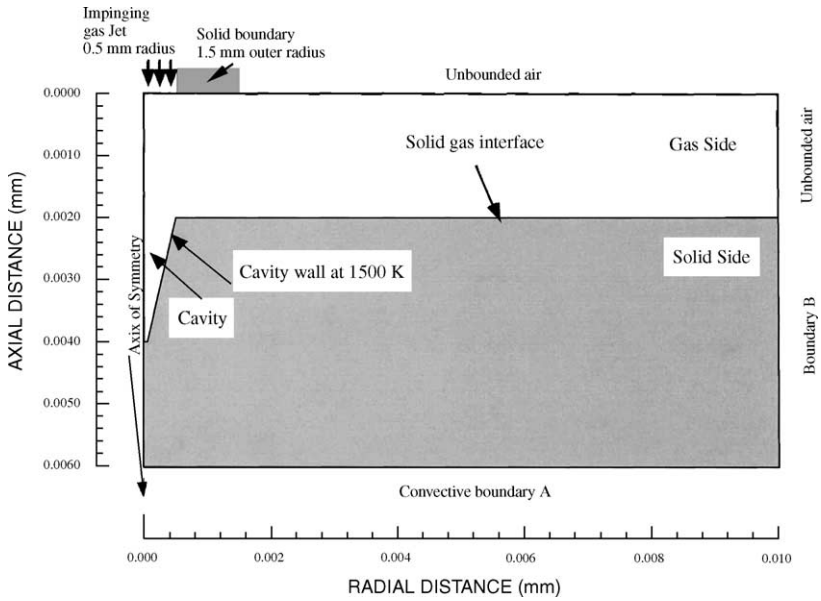

Fig. 1. A schematic view of the solution domain.

2.3. Solid boundary conditions

Two constant temperature boundaries are considered. First one is in the radial direction far away from the symmetry axis constant temperature T_{amb} (300 K) is defined (boundary A in Fig. 1). The constant temperature boundary condition is set at different locations in the radial directions at boundary A and no significant effect of T = constant was observed on the temperature and flow field in the stagnation region. Therefore, this boundary condition is set for radial distance 0.010 m from the symmetry axis. The second constant temperature boundary is set at the cavity wall (as shown in Fig. 1) T = constant (1500 K).

2.4. Solid fluid interface conditions

The coupling of conduction within the solid and convection within the fluid, termed conjugation, is required for the present analysis at the solid fluid interface. The appropriate boundary conditions are continuity of heat flux and temperature and are termed boundary conditions of the fourth kind, i.e. $T_{w_{solid}} = T_{w_{gas}}$ and $k_{solid}(\partial T_{w_{solid}}/\partial x) = k_{gas}(\partial T_{w_{gas}}/\partial x)$ and no radiation losses from the solid surface is assumed.

3. Numerical method and computation

A control volume approach is employed when discretizing the governing equations. The discretization procedure is given in [10]. The problem of determining the pressure and satisfying continuity may be overcome by adjusting the pressure field so as to satisfy continuity. A staggered grid arrangement is used in which the velocities are stored at a location midway between the grid points, i.e. on the control volume faces. All other variables including pressure are calculated at the grid points. This arrangement gives a convenient way of handling the pressure linkages through the continuity equation and is known as semi-implicit method for pressure-linked equations (SIMPLE) algorithm. The details of this algorithm is given in [11].

The computer program used for the present simulation can handle a non-uniform grid spacing. In each direction fine grid spacing near the gas jet impinging point and the hole is allocated while gradually increased spacing for locations away from the hole is considered. Elsewhere the grid spacing is adjusted to maintain a constant ratio of any of two adjacent spacing. The grid generated in the present study is shown in Fig. 2. The number of grid planes used normal to the r and x directions are 90 and 70, respectively, thus making a total of 6300 grid points. The grid independence tests were conducted and it was observed that for 90×110 grid points, the predictions were in excellent agreement with the results of 90×70 grid points, i.e., the difference in predictions is less than 0.1%. Six variables are computed at all grid points; these are: the two velocity components, the local pressure, the two turbulence quantities and the temperature.

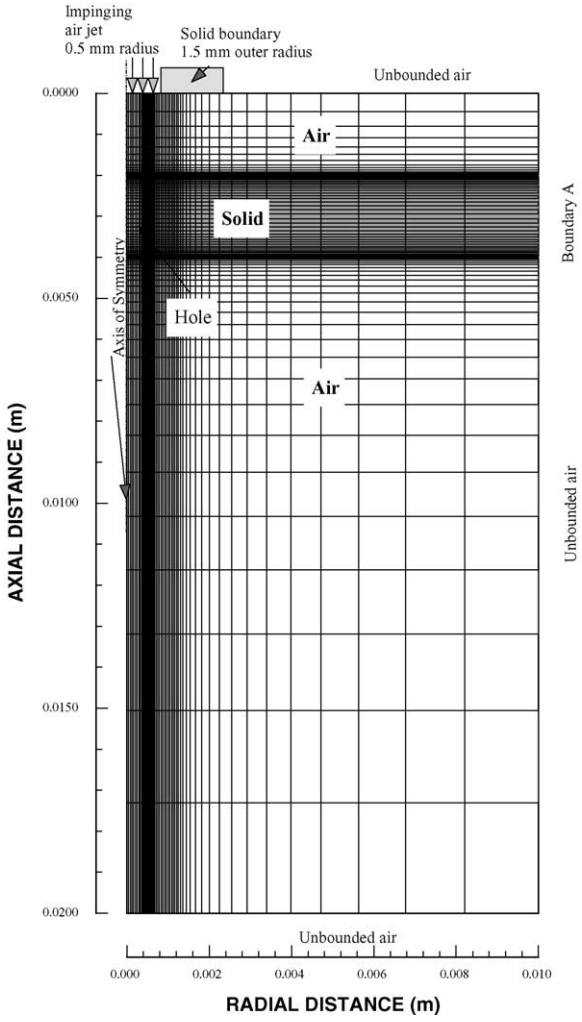

Fig. 2. Grid used in the simulations.

4. Results and discussion

Jet impingement onto a conical cavity is investigated. The cavity wall is set to the elevated temperature. This enables us to examine the influence of the thermodynamic pressure on the flow and heat transfer characteristics, A numerical solution employing a control volume approach is introduced when solving the governing equations of flow and heat transfer. The simulations are repeated for four cavity depths and two assisting gas jet velocities.

Fig. 3a shows the dimensionless velocity magnitude (V/V_j) along the symmetry axis (x/D and $r/D = 0$) is shown for two different cavity depths. Velocity magnitude reduces along the symmetry axis. The region where the velocity magnitude approaches zero indicates the stagnation region in the cavity. The influence of high thermodynamic pressure on the flow in the cavity behind the stagnation region is not considerable, since the velocity magnitude resulted from elevated and room temperature cavity wall cases are similar. This can be seen from Fig. 3b, in which

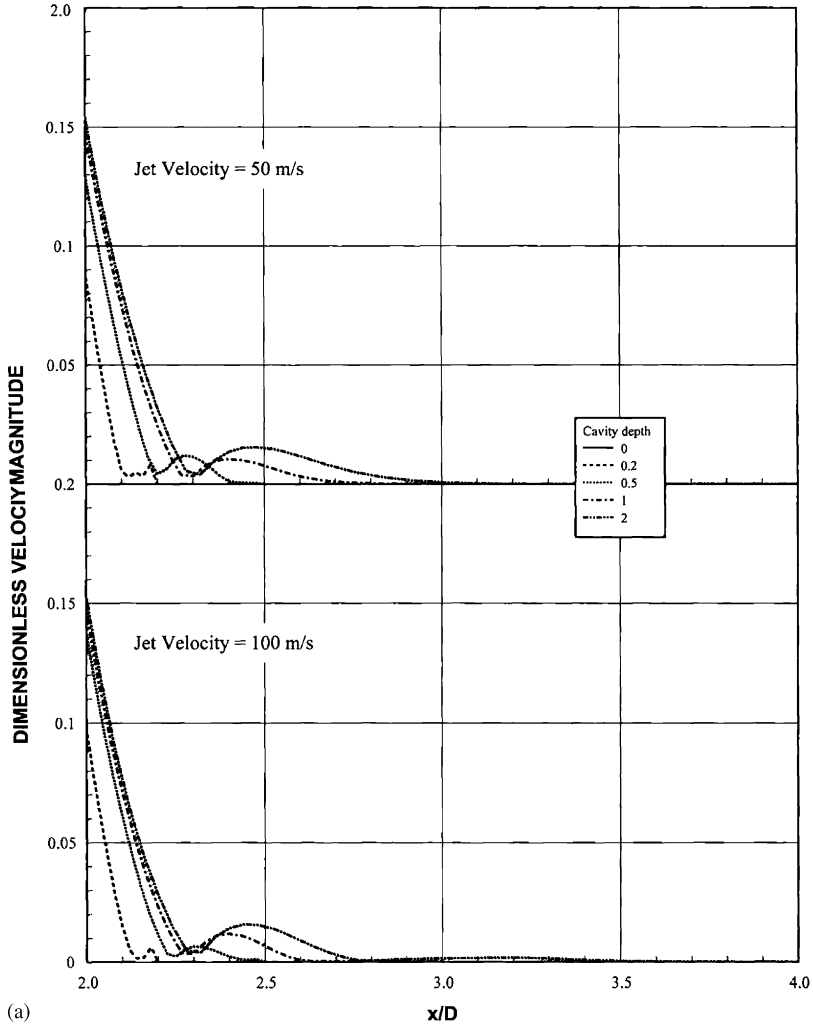

(a)

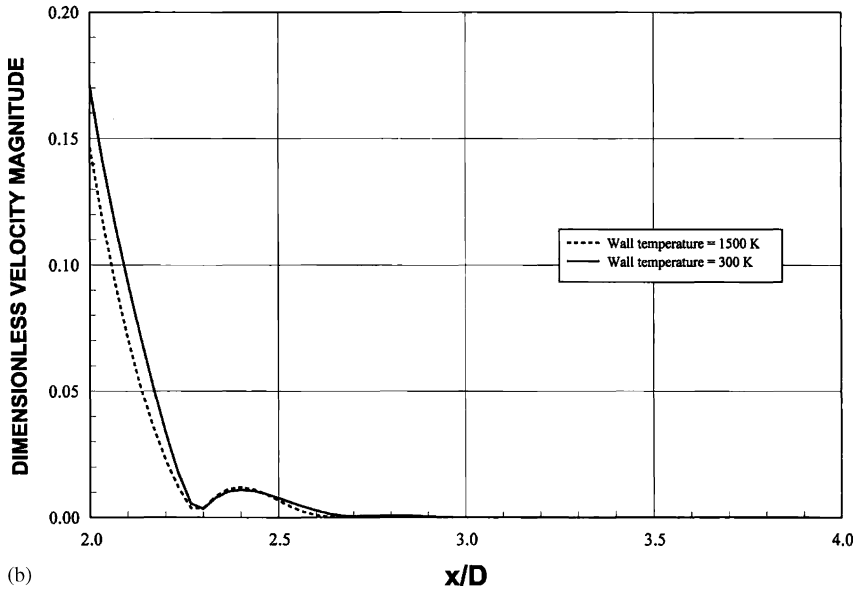

(b)

Fig. 3. (a) Dimensionless velocity magnitude along the symmetry axis. (b) Velocity magnitude along the symmetry axis for the cavity depth of $L^* = 1$ and two cavity wall temperatures.

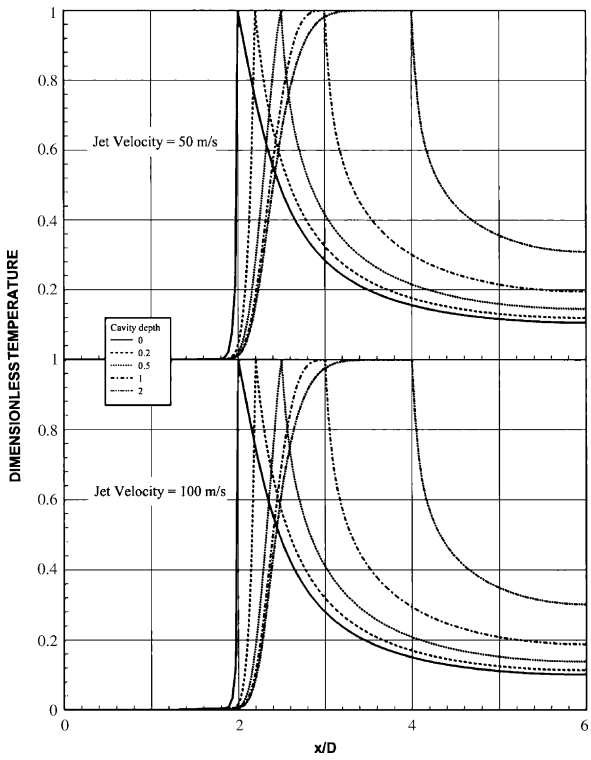

Fig. 4. Dimensionless temperature profiles along the symmetry axis inside the cavity for different cavity depths and two jet velocities.

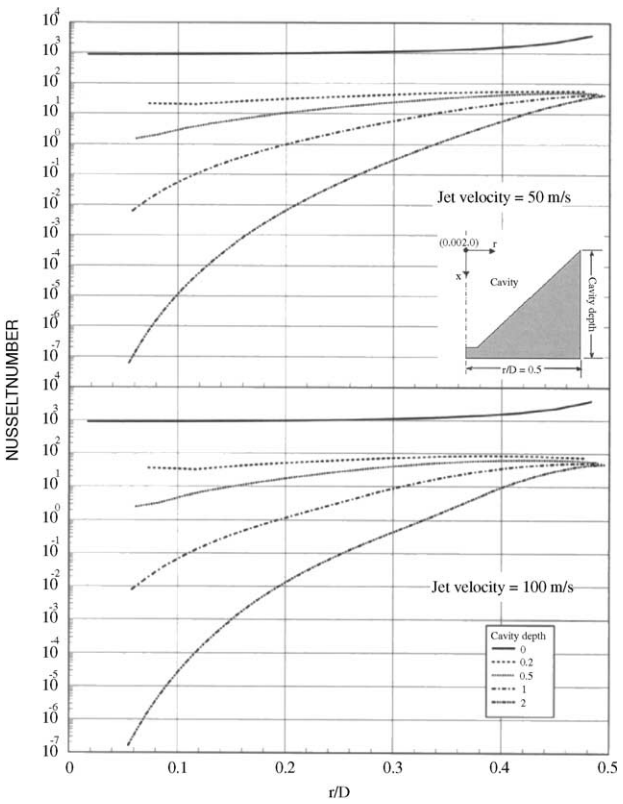

Fig. 5. The Nusselt number variation in the radial direction.

velocity magnitude is shown for the cavity depth of $L^* = 1$ and two cavity wall temperatures. It is evident that the high wall temperature reduces the velocity magnitude along the symmetry axis in the cavity provided that the location of stagnation region does not change.

Fig. 4 shows the dimensionless temperature profiles along the symmetry axis inside the cavity for different cavity depths and two jet velocities. Temperature profiles rises sharply along the symmetry axis to reach the cavity wall temperature for cavity depth <0.5 ($L^* < 0.5$). As the cavity depth increases, temperature rise becomes gradual behind the stagnation region. The gradual rise of temperature is because of the cavity flow generated in this region. Since the flow is not totally stagnant in this region, temperature of the fluid rises gradually as the distance increases from the stagnation region towards the cavity-end.

Fig. 5 shows the Nusselt number variation in the radial direction. It should be noted that $r/D = 0$ represents the symmetry axis while $r/D = 1$ corresponds to the cavity exit in the radial direction. The Nusselt number attains considerably low values at the cavity-end. This is because of the development of almost stagnation zone in this region. As the distance increases in the radial direction, Nusselt number increases sharply. This is more pronounced for deep cavities. The influence of the stagnation region formed in the cavity on the Nusselt number is not clearly observed from the curves due to logarithmic plot.

5. Conclusions

Jet impingement onto a conical cavity with elevated wall temperature is considered. A numerical scheme using a control volume approach is employed to solve governing equations of flow and heat transfer. The Reynolds stress turbulence model is accommodated to account for the turbulence. The simulations were repeated for four cavity depths and two impinging jet velocities. It is found that the stagnation region moves into the cavity as the depth increases. The influence of cavity depth on the flow field, which is generated behind the stagnation region in the cavity is considerable. The specific conclusions derived from the present work can be listed as follows:

1. Velocity magnitude reduces sharply for shallow cavities and the flow behind the stagnation region is developed in the cavity. The influence of the cavity wall temperature on the flow behind the stagnation region is not considerable along the symmetry axis.
2. Temperature profiles decays gradually in the cavity for deep cavities. This is because of the development of the flow behind the stagnation region in the cavity.
3. The Nusselt number increases gradually in the radial direction towards the cavity exit for deep cavities. The influence of the flow behind the stagnation region on the Nusselt number is more pronounced for high jet velocity (100 m/s).

Acknowledgements

The authors acknowledge the support of King Fahd University of Petroleum and Minerals, Dhahran, Saudi Arabia, for this work.

References

[1] S. Polat, B. Huang, S. Mujumdar, W.J.M. Douglas, Numerical flow and heat transfer under impinging jets: a review, Annual Review of Numerical Fluid Mechanics and Heat Transfer, vol. 126, Hemisphere Publishing Corporation, 1989, Chapter 4, pp. 157–197.
[2] K. Jambunathan, E. Lai, M.A. Moss, B.L. Button, A review of heat transfer data for single circular jet impingement, Int. J. Heat Fluid Flow 13 (1992) 106–115.
[3] J.W. Baughn, S. Shimizu, Heat transfer measurements from a surface with uniform heat flux and an impinging jet, ASME J. Heat Transf. 111 (1989) 1096–1098.
[4] J.W. Baughn, A.E. Hechanova, X. Yan, An experimental study of entrainment effects on the heat transfer from a flat surface to a heated circular impinging jet, ASME J. Heat Transf. 113 (1992) 1023–1025.
[5] G.K. Morris, S.V. Gaimella, R.S. Amano, Prediction of jet impingement heat transfer using a hybrid wall treatment with different turbulent Prandtl number functions, J. Heat Transf. 118 (1996) 562–569.
[6] B.M. Tchavdarov, Two-dimensional vortex dynamics of inviscid–viscous interaction at turbulent gas jet impingement, Int. J. Heat Fluid Flow 18 (1997) 316–327.
[7] R.S. Amano, H. Brandt, Numerical study of turbulent axisymmetric jets impinging on a flat plate and flowing into an axisymmetric cavity, ASME J. Fluids Eng. 106 (1984) 410–417.
[8] B.E. Launder, W. Rodi, The turbulent wall jet—measurement and modeling, Annu. Rev. Fluid Mech. 15 (1983) 429–433.
[9] P. Bradshaw, T. Cebeci, J.H. Whitelaw, Engineering Calculation Methods for Turbulent Flow, Academic Press, 1981, p. 51.
[10] H.K. Versteeg, W. Malalasekera, An Introduction to Computational Fluid Dynamics, The Finite Volume Method, Longman Scientific and Technical, 1995.
[11] S.V. Patankar, Numerical Heat Transfer, McGraw-Hill, 1980.